

A10

High Statistic Study of the Reaction $p + W \rightarrow \mu^+ + \mu^- + X$ at $\sqrt{s} = 27$ GeV

Presented by P. M. MOCKETT

Michigan-Northeastern- Washington Collaboration

Results from a high statistic study of the reaction $p + W \rightarrow \mu^+ + \mu^- + X$ at $\sqrt{s} = 27$ GeV are presented. Over 275,000 events with a dimuon mass greater than 6 GeV were reconstructed and an enhancement above the continuum of 15,000 events was observed at the Y mass region. The continuum spectrum falls approximately as $e^{-1.4 * 0.4 (GeV)}$. No enhancements except in the Y region are observed. The very large acceptance of the apparatus enables an accurate measurement of the mass (M), transverse momentum (p_T) and Feynman $X(X_F)$ dependence of the dimuon pair. The p_T spectrum from 0 to 4 GeV is

fitted exceedingly well by the function $dN/dM dX_F dp_T \propto T^6$ for $6 < M < 14$ GeV and $0 < X_F < 0.6$. The fitted parameter, p_0 shows no dependence on X_F or p_T interval at about the 5% level. p_0 also shows little dependence on M although a modest increase at the Y mass is observed. With further study of the experiment's systematic effects, the error on p_0 may be reduced to the statistical error level of about 1%. The average value of $|X_F|$ as a function of mass shows no significant difference between continuum masses of $M \ll 7$ and $M \approx 13$ GeV but there is a decrease in the average value in the Y mass region.

A 10

A Study of High Mass e^+e^- Pairs Produced in p-p Collisions at the CERN ISR

Presented by L. CAMILLERI

CERN-Columbia-Oxford-Rockefeller Collaboration

An apparatus consisting of a superconducting solenoid cylindrical drift chambers and two arrays of lead glass Cerenkov counters have been used at the CERN ISR to study the production of e^+e^- pairs of invariant mass larger than $6 \text{ GeV}/c^2$. The apparatus is shown in Fig. 1. The rms momentum resolution of the drift-chamber-magnet system is given by $\Delta p_T/p_T \sim 0.07 p_T$ whereas the rms energy resolution of the lead glass is given by $\Delta E/E = 0.05 + 0.077 V' E$. The following cuts were applied to the data in order to reduce the hadronic background.

a) A track was required to point to an energy cluster in the lead glass of extent less

than or equal to 3×3 blocks.

b) The momentum of the track was required to be compatible with the energy measured in the lead glass.

c) Forming the invariant mass of a candidate electron track with all other tracks in the event, in turn, the candidate was rejected if any of these combinations gave an effective mass smaller than $160 \text{ MeV}/c^2$.

d) At least one of the two B counters traversed by the tracks was required to have recorded a pulse height greater than $1.5 \times$ single ionization.

The mass spectra, as computed using the lead glass information, of the 79 events of

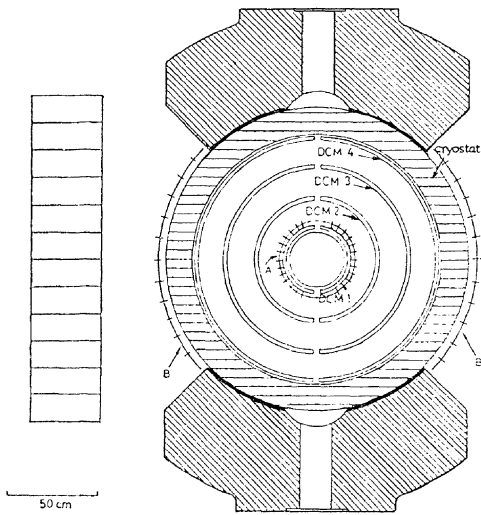


Fig. 1.

opposite charge and of the 23 events of same charge surviving the cuts are shown in Fig. 2. The background in the opposite charge distribution is taken to be equal to the same charge distribution. The differential cross-section $d^2\sigma/dm dy|_{y=0}$ are shown in Fig. 3 as a function of mass. The agreement is good with a fit to the Fermilab $V s = 27 A$ dimuon data scaled up to $V s = 62.4$ according to $m^3\text{-rfV}/dmdy|_{y=0} = F(M/V s)$.

Assuming the 15 events in the range $8.75 < M < 11.0 \text{ GeV}/c^2$ to be due to the Y resonances the cross-section for these resonances is found to be $B\text{-doldy}|_{y=0} = (1 \pm 2.0) \times 10^{-36} \text{ cm}^2$. The value of $\langle p_T \rangle$ is calculated to be $1.67 \pm 0.21 \text{ GeV}/c$ for $6 < M < 8.75 \text{ GeV}/c^2$ and $1.65 \pm 0.20 \text{ GeV}/c$ for $M > 8.75 \text{ GeV}/c^2$. The mean multiplicity of tracks associated with an e^+e^- pair is observed to be 6.1 ± 1.0 and 5.5 ± 1.0 for the two mass intervals above. The corresponding multiplicity of tracks associated to $\pi^0\pi^0$ in the same two mass intervals is found to be lower 10.0 ± 0.2 and 9.5 ± 0.2 respectively. The p_T spectrum of the tracks associated with the e^+e^- events falls off more steeply than the corresponding spectrum for $\pi^0\pi^0$ events.

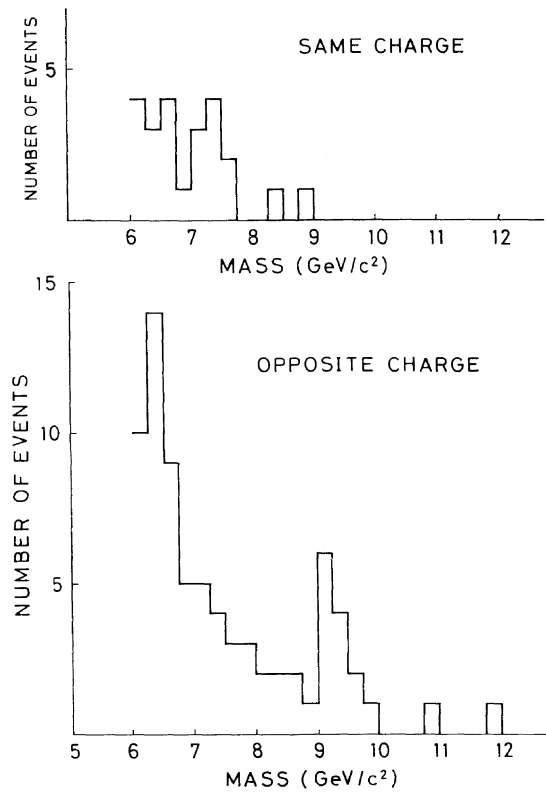


Fig. 2.

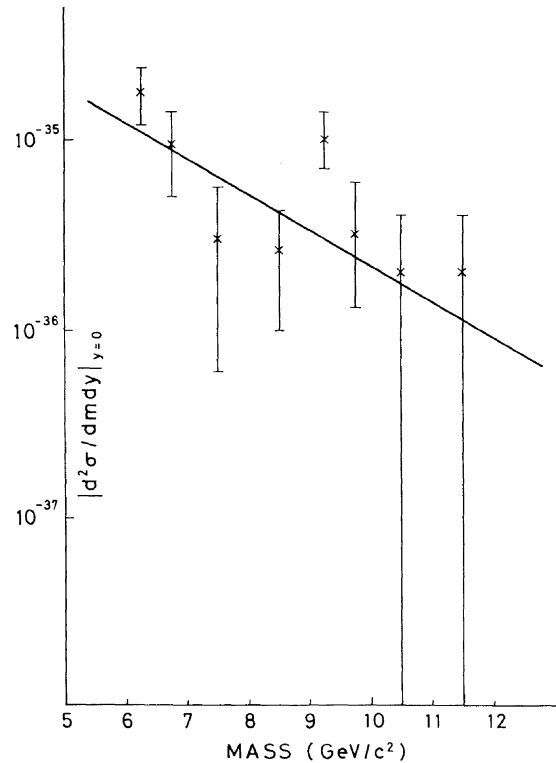


Fig. 3.

Electron Pairs Production at the ISR

Presented by I. MANNELLI

A thens-BNL-CERN-Syracuse- Yale Collaboration

An experiment is in progress at the CERN Intersecting Storage Rings to identify and measure electron pairs, produced in proton-proton collisions up to $\sqrt{s} = 63$ GeV. The pairs are detected using four modules, consisting of proportional chambers, plastic scintillator hodoscopes, lithium foil transition radiators followed by Xe-CO₂ linear proportional chambers—for the X-rays—and finally of a 17 rad. lengths liquid argon calorimeter, suitably segmented in the lateral and longitudinal direction.¹ Each module covers 50° to 130° in polar angle and 40° of azimuth.

As explained in^{2,3} background arising from external or internal photon conversions, from hadrons producing showers in the calorimeter and from chance overlap of hadron tracks with photon showers can be effectively reduced by imposing requirements on the signals available from the detectors. We estimate the efficiency ϵ for electron pair events to pass each set of requirements by observing

its effect on the J/ψ signal, which has a background that can be reliably subtracted even for the most loosely cut samples ($\epsilon = 0.43$). The results of these estimates agree well with direct determinations obtained from calibration exposures of a complete module to a test beam of known particles. The number of events observed in various mass intervals, after corrections for the efficiency ϵ , is shown in Fig. 1.

The horizontal scale has been chosen in such a way that the points for the mass interval 1.1-2 GeV, consisting essentially of background, fall on a straight line. For a pure electron pair sample one would expect values independent of ϵ , within statistics.

That is in fact what happens in the 2.8-3.4 GeV (J/ψ) region for $\epsilon < .36$ and, for the full used range of ϵ , for events with mass above 8.7 GeV (i.e., T and higher mass region).

For J/ψ at $\epsilon = .19$ the background is calculated to be $\sim 6\%$ and for the >8.7 GeV mass region the background is $\sim 6\%$ for $\epsilon = .36$.

The raw mass spectra in the J/ψ region and above 6 GeV are shown in Figs. 2 and 3a for $\epsilon = .19$. In Fig. 3b the high mass region is

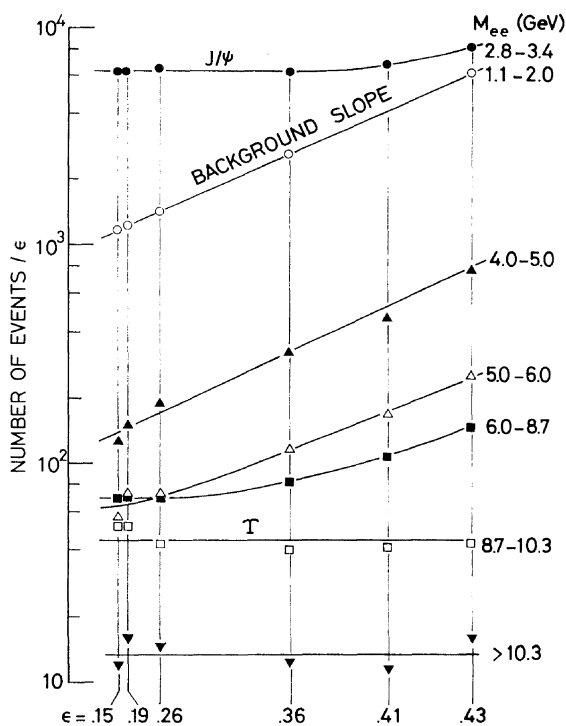


Fig. 1.

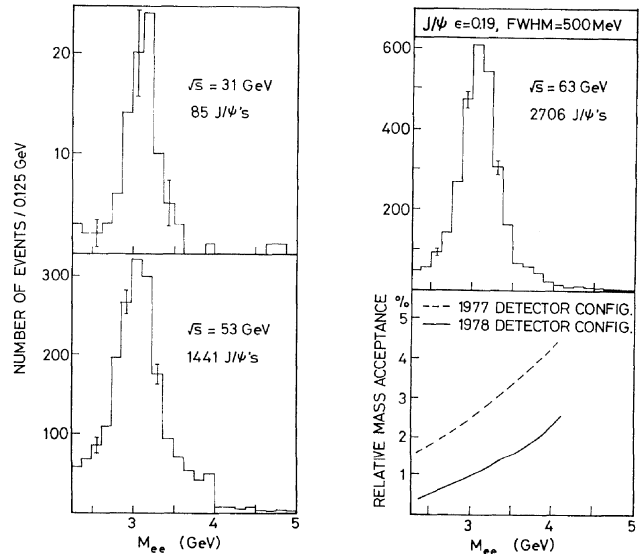


Fig. 2.

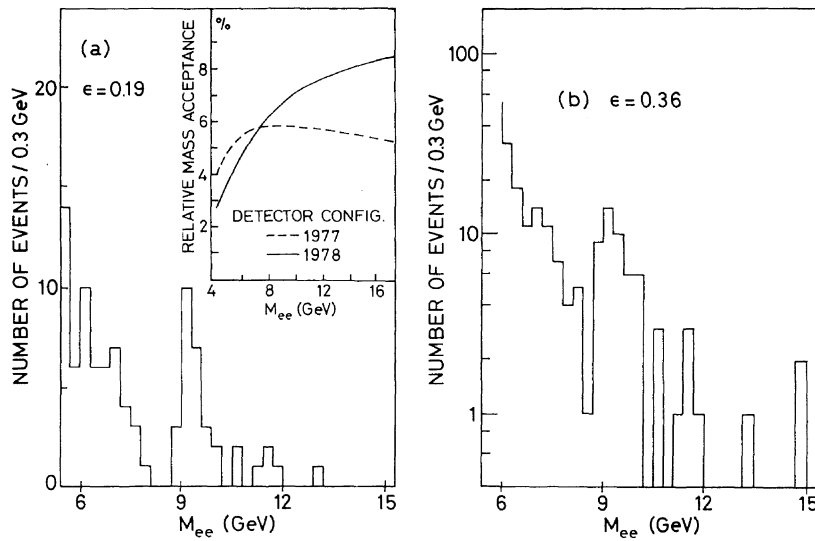


Fig. 3.

shown again on log scale for the less str identification requirements with $\epsilon=0.36$.

The 8.7-10.3 region in Fig. 3b contains 41 events. We estimate a background of 2.5 events and, by extrapolating the continuum from the region 6 to 8.7 GeV following the m/Vs dependence form ref. 4, we evaluate an electron pair continuum of about 8 events.

The mass resolution is calculated to be $a_M = 380$ MeV at the T mass, from the experimental

width of the J/ψ .

Relative values of the P_T acceptance of the apparatus have been calculated, using a Monte Carlo program which takes into account the known geometry and incorporates the threshold behaviour of each calorimeter, measured directly using events recorded without demanding *a priori* a trigger from that calorimeter. It assumes flat rapidity and isotropic decay.

Figure 4 present the acceptance corrected

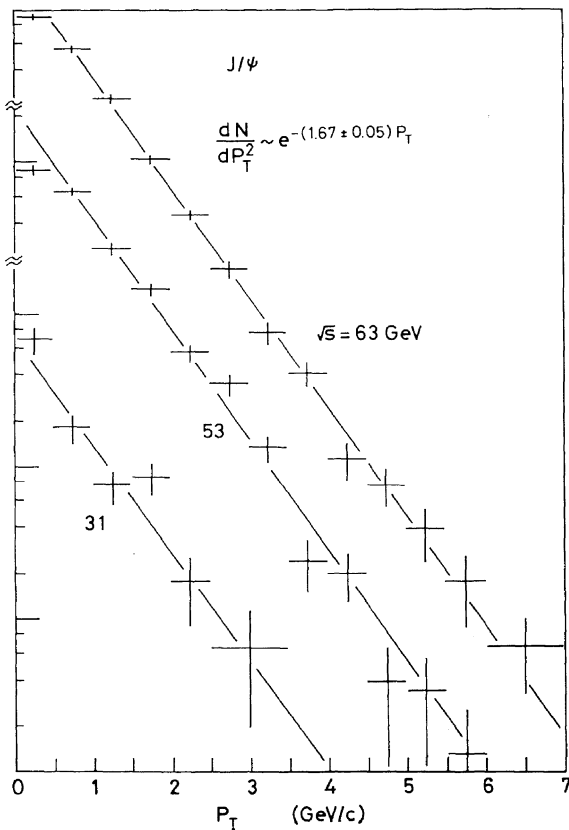


Fig. 4.

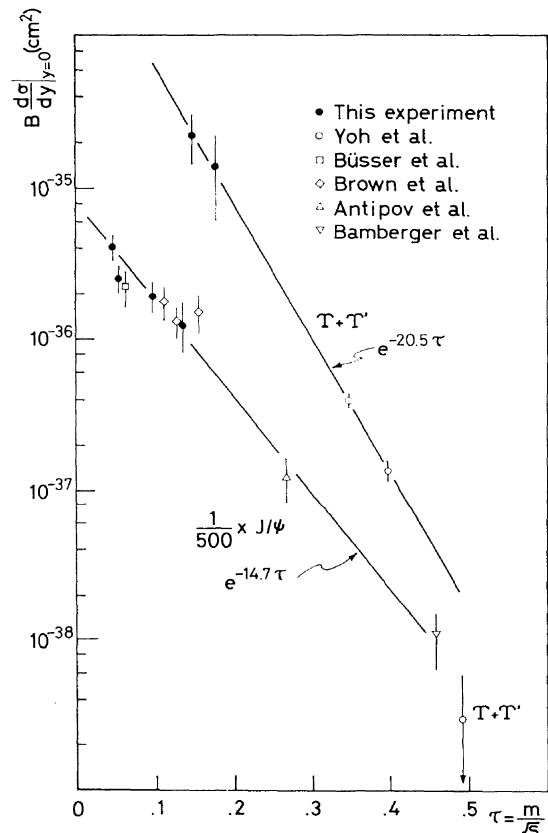


Fig. 5.

Table I.

\sqrt{s} [GeV]	\mathcal{L} [10^{36} cm^{-2}]	# Events $J/\psi \rightarrow ee$	b parameter [GeV^{-1}] $d\sigma/dP_{\perp}^2 \propto e^{-bP_{\perp}}$	$\langle P_{\perp} \rangle_{FIT} = 2/b$ [GeV/c]	$B(d\sigma/dy) _{y=0}$ [10^{-33} cm^2]
31	0.91	77 ± 10	1.64 ± 0.23	$1.22 \pm .17$	9.64 ± 2.30
53	8.20	754 ± 35	1.68 ± 0.04	$1.19 \pm .03$	12.58 ± 2.58
63	23.89	2286 ± 70	1.67 ± 0.03	$1.20 \pm .02$	20.53 ± 4.15

 Table II. γ region (8.7–10.3 GeV).

\sqrt{s} [GeV]	Number of events	Background estimate #ev.	Continuum estimate #ev.	Signal -continuum #ev.	$B(d\sigma/dy) _{y=0}$ [10^{-36} cm^2]	Luminosity [10^{36} cm^{-2}]
53	9	0.5	1.7	6.8 ± 3.7	14 ± 8	14
63	32	2	6.2	23.8 ± 7	22 ± 8	26.5

ANI6.PT distribution for the J/ψ . All points for $P_{\perp} > .5 \text{ GeV}/c$, in the P_T range which extends up to $7 \text{ GeV}/c$ at $V_s = 63 \text{ GeV}$, follow well an exponential law vs P_T with slope $b = 1.67 \pm 0.05 \text{ (GeV}/c)^{-1}$ independent of V_s . The corresponding $\langle P_{\perp} \rangle$ calculated from the fit is $2/b = 1.20 \pm 0.04 \text{ GeV}/c$. Also in the γ region, within the relatively large statistical error, the exponential fit continues to be adequate and produces the slope $b = 1.2 \pm 0.13 \text{ (GeV}/c)^{-1}$ and $\langle P_{\perp} \rangle = 1.67 \pm 0.18 \text{ GeV}/c$.

The cross section values for the J/ψ and Y are listed in Tables I and II.

The errors quoted for $B \cdot d\sigma/dy|_{y=0}$ include, in addition to the statistical errors, the estimated 20% systematic uncertainty from run to run at different V_s .

Figure 5 shows the data plotted vs m/V_s . The line shown on the J/ψ data is from ref. 4. It should be remarked that the relative lack of experimental points, with sufficiently small errors at large values of m/V_s , leaves some freedom to its slope. The line drawn through the Y points is an eye-ball fit and appears to be somewhat steeper than the J/ψ line. In fact at the weighted average $V_s = 60 \text{ GeV}$, $B \cdot d\sigma/dy|_{y=0}$ (integrated from 8.7 to 10.3 GeV,

* The value of the slope $b = 1.67 \pm 0.05 \text{ (GeV}/c)^{-1}$ we find for $dN/dP_T^2 \sim e^{-bP_T}$ for J/ψ can be compared with the result $b = 1.51 \pm 0.12 \text{ (GeV}/c)^{-1}$ of ref. 8, over the P_T range 0-2 GeV/c.

after continuum subtraction) is about 50 times higher than the corresponding sum for the Y and Y' measured⁷ at $V_s = 21$. It is also interesting to remark that the ratio of resonance to continuum contribution, in the mass interval 8.7-10.3 GeV, is estimated to be 4 to 1 at $V_s = 60$ compared with about 1 to 1 at $V_s = 27$,^{7,9} over the same mass interval.

References

1. J. H. Cobb *et al.*: A liquid argon shower detector for an ISR experiment. Submitted to Nuclear Instruments and Methods.
2. J. H. Cobb *et al.*: Phys. Letters **68B** (1977) 101; C. Kourkoumelis: CERN 77-06 (1977).
3. J. H. Cobb *et al.*: Phys. Letters **72B** (1977) 273.
4. M. J. Schochet: Review of dilepton production at high energy in hadron-hadron collisions, EFI, 77-66 (1977).
5. A. Bamberger *et al.*: Nucl. Physics **B134** (1978) 1; Yu. M. Antipov *et al.*: Phys. Letters **60B** (1976) 309; K.J. Anderson *et al.*: Phys. Rev. Letters **36** (1976) 237; H. D. Snyder *et al.*: Phys. Rev. Letters **36** (1976) 1413; F. W. Busser *et al.*: Phys. Letters **56B** (1975) 482.
6. S. W. Herb *et al.*: Phys. Rev. Letters **39** (1977) 252.
7. J. K. Joh *et al.*: Study of scaling in hadronic production of dimuons, Fermilab Pub. 78/52 Exp.
8. C. B. Brown *et al.*: Preprint Fermilab 77/54-Exp, Study of J/ψ and $\langle p' \rangle$ production in proton-nucleus collisions with electron and muon pairs.
9. D. M. Kaplan *et al.*: Phys. Rev. Letters **40** (1978) 435.

A 10 Measurement of High-Mass Muon Pairs at Very High Energies

Presented by H. NEWMAN

CERN-Harvard-Fraseati-MIT-Naples-Pisa Collaboration

We present preliminary data¹ on the reaction:

$$p + p \rightarrow \mu^+ \mu^- + X$$

at a center of mass energy of 63 GeV for muon pair masses of 3 to 20 GeV, from experiment R209 at the CERN Intersecting Storage Rings.

The detector covers $15^\circ < \theta < 110^\circ$ ($-0.3 < x < 0.9$) with essentially complete ϕ coverage. It consists of a large array of magnetized Fe toroids, drift chambers and hodoscopes (Fig. 1) which cleanly selects muon pairs and filters

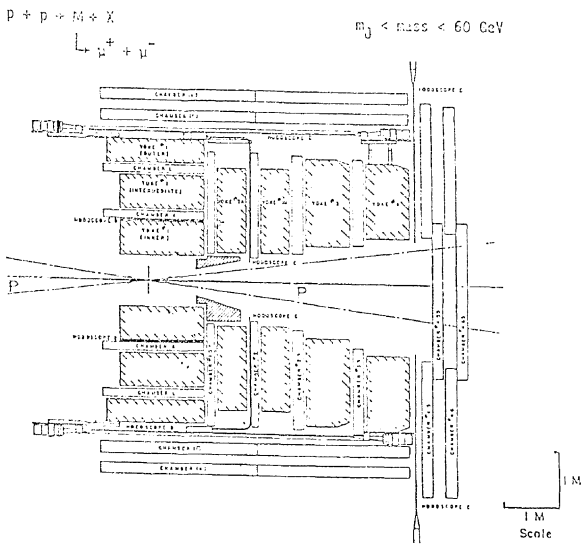


Fig. 1.

out hadron background, complemented by a central detector of drift chambers and hodoscopes which sorts out the high-multiplicity associated hadrons. The muons are bent mainly in ϕ by the toroids, which provide a generally azimuthal field of 18 K Gauss, and $J \approx 26 \text{ KG-m}$ at 90° . The mass resolution (Δ) is $\Delta M/M \approx 10\%$, limited by multiple scattering.

The trigger requires >2 of each of the outer, intermediate, and inner hodoscope elements to fire. The outer and intermediate hodoscopes are divided into ϕ sectors of $\approx 15^\circ$, and the elements struck by each muon must correspond in ϕ within ± 1 sector. After

applying TOF cuts on cosmic-ray muons and single-beam backgrounds, using the outer counters and auxiliary veto counters near the ISR beams, the trigger decision is given over to a programmable microprocessor. This device performs refined checks on the above criteria, and searches for at least 6 crude space points in the large drift chambers. At a luminosity of $10^{31} \text{ cm}^{-2} \text{ sec}^{-1}$ the final trigger rate is typically 0.4 Hz.

The mass acceptance for a muon pair has been computed by a detailed Monte Carlo program. It is flat above $M_{\mu\mu} \approx 6 \text{ GeV}$ at a level of $\approx 16\%$ of 4 Trsr^{-1} . Below 6 GeV the acceptance falls smoothly to 50% of the plateau value at $\approx 5 \text{ GeV}$ and to $< 1\%$ at the mass of the J/ψ . As the x_F and p_T distributions are still being analyzed in our data, we assumed that the mu-pairs are produced according to the J/ψ -production x_F and p_T distributions measured at Fermilab by Anderson *et al.*,²

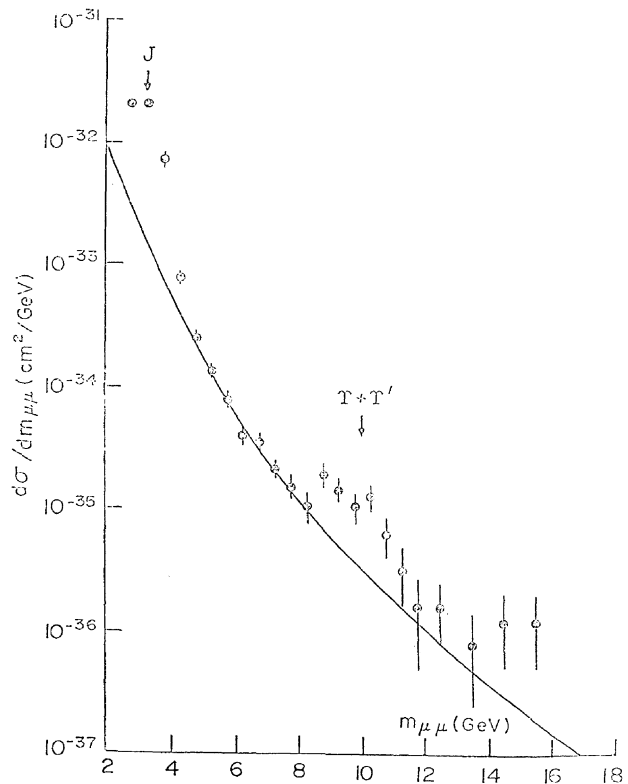


Fig. 2.

with a uniform decay distribution $\rightarrow \gamma \gamma$. In spite of this model dependence, because of the large geometrical acceptance of the detector, the cross-section we present here could be correct within a factor of 2 for $4 < m_{\gamma\gamma} < 13$ GeV. The cross-section in our preliminary analysis is not precise for the $\gamma \gamma$, because of the small acceptance at this mass value.

Figure 2 shows the acceptance-corrected mass spectrum $d\sigma/dM_{\gamma\gamma}$ corresponding to a time-integrated luminosity of $2.6 \times 10^{37} \text{ cm}^{-2}$. The low mass data is dominated by $\gamma \gamma$ production, while for $8 < M_{\gamma\gamma} < 11$ GeV the spectrum is dominated by Y and T' production, where the latter structure is observed to have a width in reasonable agreement with the computed mass resolution. The solid curve in Fig. 2 is a zero parameter scaling model prediction based on the Drell-Yan mechanism, which Kinoshita, Satz and Schildknecht³ (KSS) have found to

be in agreement with the Columbia-Fermilab-Stony Brook data (CFS).⁴ The agreement between our data and the scaling prediction of KSS is quite striking, particularly in light of the fact that our measured cross-section is a factor of 15 higher at 5 GeV mass, to a factor of 200 higher at 12 GeV mass, compared to the lower energy CFS data.

References

1. Paper submitted to this Conference by the CERN-Harvard-Frascati-MIT-Naples-Pisa Collaboration. Refer to this paper and the references therein.
2. Anderson *et al.*: Phys. Rev. Letters 37 (1976) 799.
3. Kinoshita, Satz, and Schildknecht: report BI-TP 77/14 (1977).
4. Herb *et al.*: Phys. Rev. Letters 39 (1977) 252; see also paper No. 732 submitted to this Conference.

A 10 Electron-Pair Production at the CERN ISR

Presented by M. BANNER

CERN-Saclay-Zurich Collaboration

A double arm spectrometer, located one on each side of the ISR interaction region detects the electron pairs around 90° of the beams direction. The element of each spectro-

meter (Fig. 1) are a magnet for charge and momentum measurement, a Cerenkov counter air filled located in the magnet for electron identification and a lead glass array for further

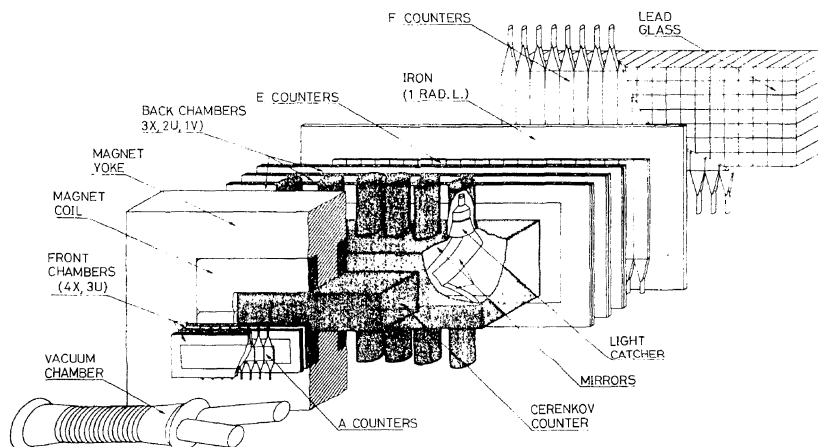


Fig. 1.

electron identification. For trigger purposes, a threshold of 600 MeV on each electron was imposed. The Cerenkov is segmented in 12 cells and allows an association between the track direction and the Cerenkov cell. The electron pair mass can be determined from the momenta measurement or from the lead glass measurements. Figures 2 and 3 show the corresponding spectra. A clear J/ψ signal can be seen and the measurement

errors can therefore experimentally estimated. The requirement that the momentum and the energy measurement agree within 2 standard deviation leads to the spectrum of Fig. 4. The background is monitored by the same sign electron pair and is negligible above 3 GeV mass. The electron-pair detection efficiency in these conditions is 0.5 and Fig. 5 shows that we have good agreements with other data for the J/ψ production. No electron

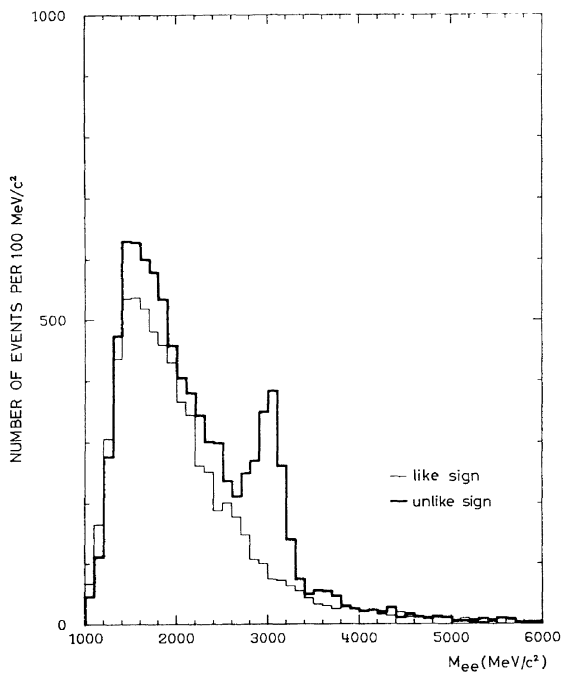


Fig. 2.

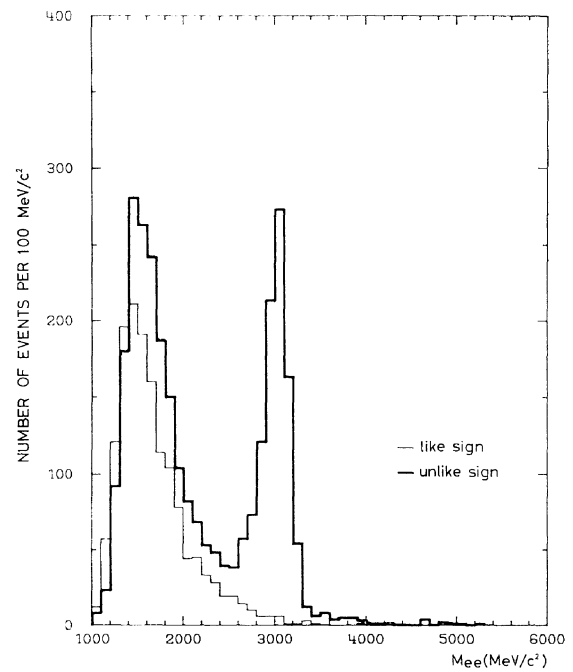


Fig. 4.

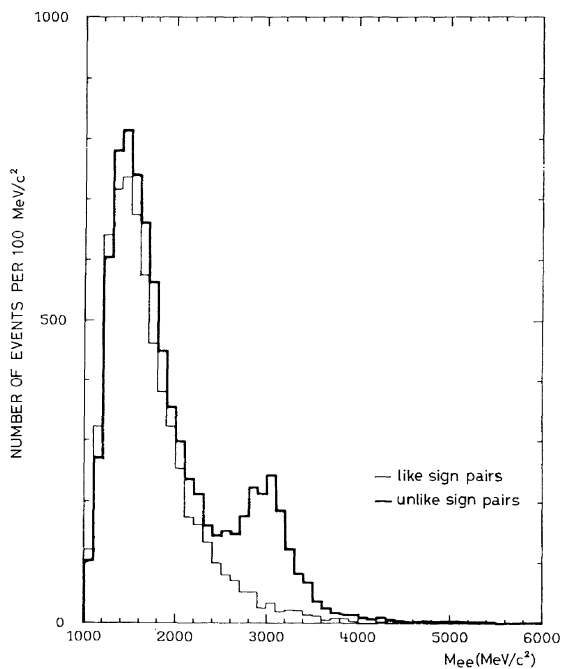


Fig. 3.

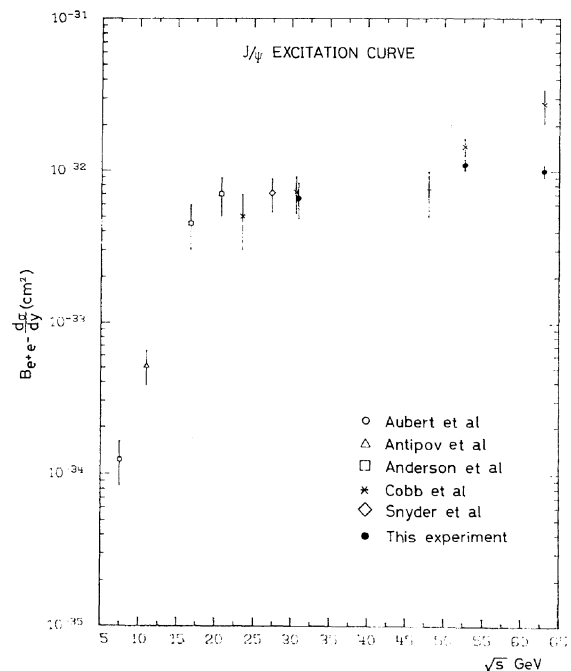


Fig. 5.

pairs was found above 6 GeV mass for an integrated luminosity of $1.5 \cdot 10^{37}$. Taken into account the acceptance of our apparatus, the cross section $B'dajdy|_{y=0}$ to produce the T 's to 90% confidence level less than $20 \cdot 10^{-36}$.

With 30% more data analyses, one event at 7 GeV mass and one event at 9.4 GeV mass was found. One event corresponds to a cross section $B-da/dy|_{y=0}$ of $5.5 \cdot 10^{-36}$.

PROC. 19th INT. CONF. HIGH ENERGY PHYSICS
TOKYO, 1978

A 10 Production of High Mass Muon Pairs by Pion Beams

K. J. ANDERSON

Enrico Fermi Institute, University of Chicago, Chicago, Illinois 60637

Introduction

The purpose of this talk will be to review the experimental data on production of high mass muon pairs by pion beams. I will focus on the continuum region above and below the J/ψ and will attempt to show the data are consistent with the hypothesis that the dominant production mechanism is through the annihilation of a quark-antiquark pair (qq)-the Drell-Yan model.¹ Based on this assumption I will show the results of a first attempt to extract information on the pion structure from muon pair data.

I will also show some new data on the production of the $(p^f$ and ρ^0 states.

Cross Section Ratios

The first piece of evidence for the qq annihilation model is the asymmetric rates of production of continuum pairs by π^+ and n^+ beams off carbon, an isoscalar target. A hadronic production mechanism would yield equal cross sections. The Drell-Yan model predicts that the cross section ratio

$$\frac{\sigma(n^+ C \rightarrow j\mu^+ j\mu^- + X)}{\sigma(\pi^+ C \rightarrow j\mu^+ j\mu^- + X)}$$

should approach 1/4 at large values of $M_{\mu\mu}^2/s$ where valence quarks dominate. The valence quarks of the TC^+ or TZ^- provides a single d or \bar{u} antiquark, respectively, which annihilates with one of the symmetric set of u and d quarks in the carbon target. One then expects

the cross section ratio to reflect only the ratio of the square of the annihilating quark charges yielding 1/4. Data from Fermilab at 225 GeV/c are shown in Fig. 1a.² The ratio

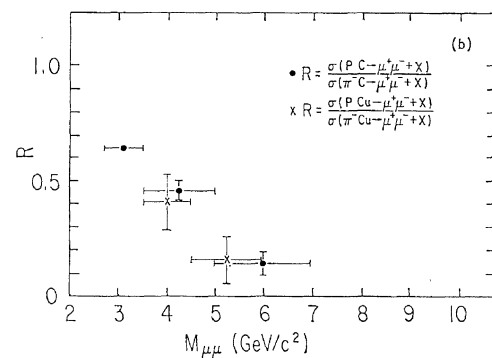
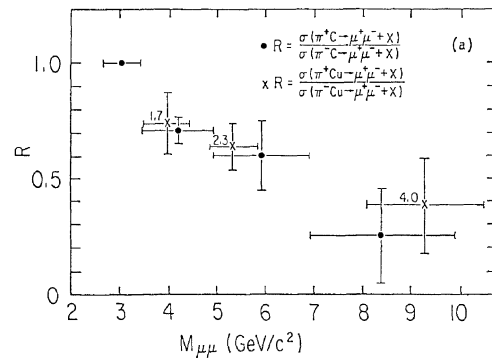


Fig. 1 a. Cross section ratio for $\hat{I}Z^+$ and TZ^- produced muon pairs as a function of the pair mass. Carbon target data at 225 GeV/c are from ref. 2. Copper target data at 40 GeV/c are from ref. 3 and has been plotted at equivalent M^2/s values. True mass values are listed on the data points, b. Proton to x^- ratio as above.

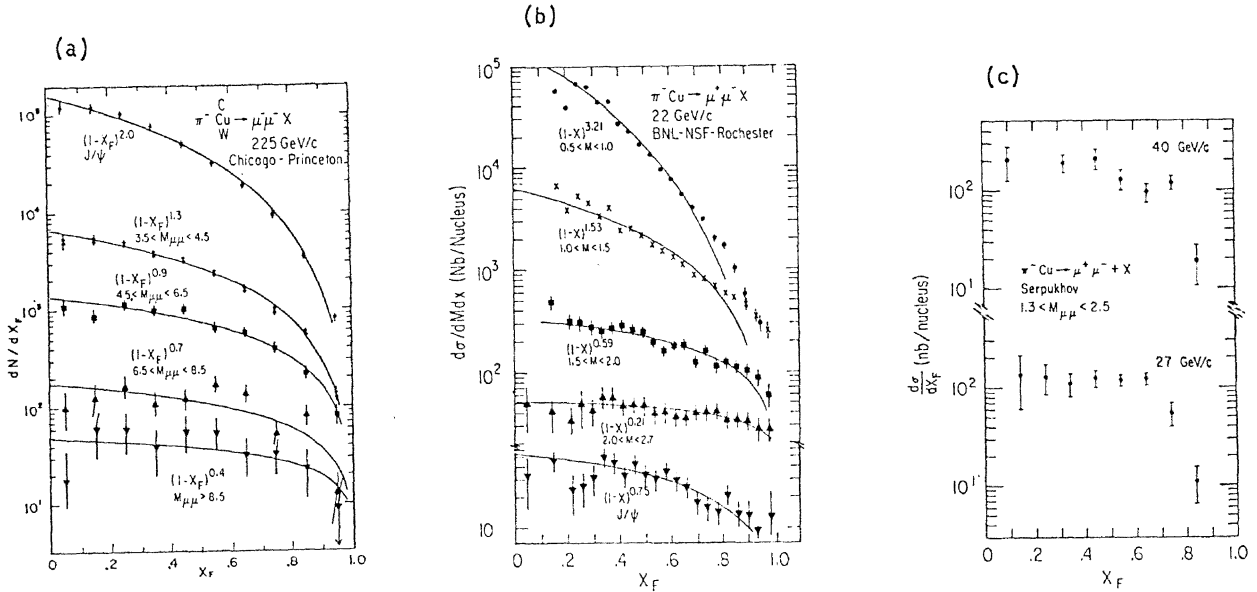


Fig. 2. a. x_p dependence versus mass for π^- induced data at 225 GeV/c from ref. 1.
 b. rr induced data at 22 GeV/c from ref. 4.
 c. x_F dependence for pairs in the mass interval $1.3 < M_{\mu\mu} < 2.5$ for 27 GeV/c and 40 GeV/c rr induced data from ref. 5.

decreases asymptotically toward the expected value. Also shown on the figure are copper target data at 40 GeV/c from CERN.³ The 40 GeV/c data have been plotted at an equivalent M^2/s value. As is expected, the cross section scales.

The ratio

$$\frac{\sigma(pC \rightarrow \mu^+ \mu^- + X)}{\sigma(\pi^- C \rightarrow \mu^+ \mu^- + X)}$$

should approach zero by these arguments since the proton has no valence antiquarks. The data are shown in Fig. 1b. The ratio tends toward zero as is predicted.

x Dependence

The x_F dependence of muon pairs produced in $\pi^- N$ interactions shows a pronounced flattening with increasing mass as is shown in Fig. 2a for data at 225 GeV/c. Data at 22 GeV/c exhibit a similar trend at equivalent M^2/s values as is seen in Fig. 26.⁴ Serpukhov data (Fig. 2c) at 27 GeV/c and 40 GeV/c for muon pairs between 1.3 and 2.5 GeV/c² has a flatter dependence at the lower s (larger M^2/s)

p_T Dependence

At 225 GeV/c the $\langle p_T \rangle$ of muon pairs raises with increasing mass up to masses of 4 GeV/c². Above 4 GeV/c² the $\langle p_T \rangle$ is con-

stant (Fig. 3). Also shown in Fig. 3 are $\langle p_T \rangle$ data from proton induced events at 200 GeV/c. At saturation, the pion data have a larger $\langle p_T \rangle$ value. In an equivalent M^2/s range, lower energy data have not reached a plateau in $\langle p_T \rangle$.

No substantial correlation in x_F and $\langle p_T \rangle$ is

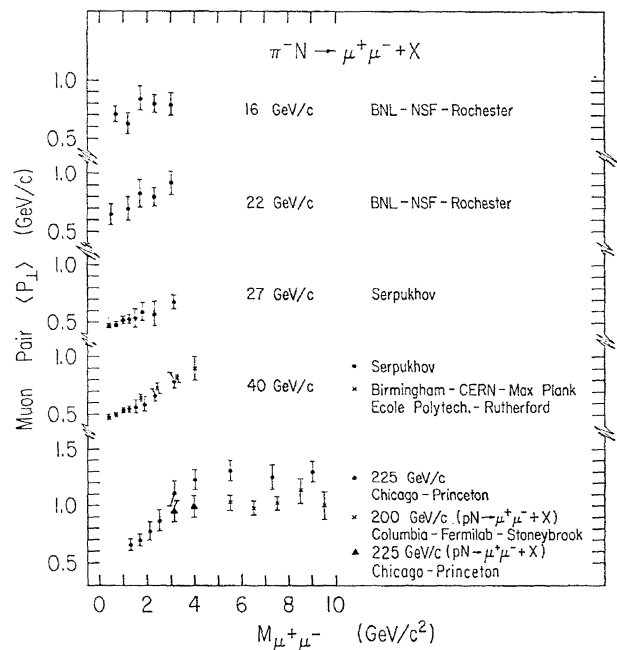


Fig. 3. Mean transverse momentum of pairs vs pair mass for π^- induced pairs from 16 to 225 GeV/c from refs. 2-5. For comparison, data from proton induced pairs at 200 GeV/c are also shown (ref. 11).

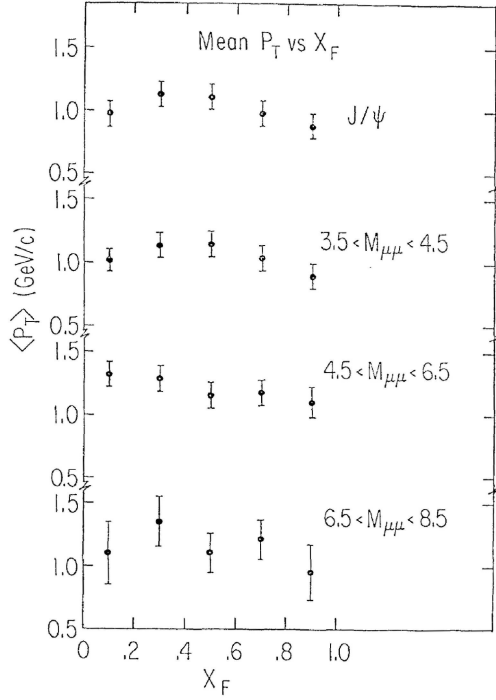


Fig. 4. Variation of muon pair mean transverse momentum with x_F for various mass regions. The data are for π^- -induced pairs at 225 GeV/c from ref. 2.

seen in the 225 GeV/c data (Fig. 4).

Angular Distribution

The decay angle distribution of the muon pair in its rest frame should go as:

$$\frac{d\sigma}{d\cos\theta^*} = \alpha (1 + \cos^2\theta^*)$$

where θ^* is the angle between muons and annihilating quark pair directions. When the pair p_T is zero, the beam and target direction define the quark pair direction. When p_T is nonzero the quark direction is not determined. Choosing the mean angle between the target and the negative of the beam direction in the pair center of mass as the reference direction has been suggested by Collins and Soper.⁶ The angle between the decay muon direction and this reference direction, θ_{es} , attempts to average p_T effects. The distribution of $\cos\theta_{es}$ is shown in Fig. 5 for J/ψ events and for muon pairs in the continuum above the J/ψ from data at 225 GeV/c. The data show a sharp contrast between J/ψ and continuum pairs. No evidence of polarization is seen in J/ψ events. The continuum shows the polarization expected for production by qq annihilation.

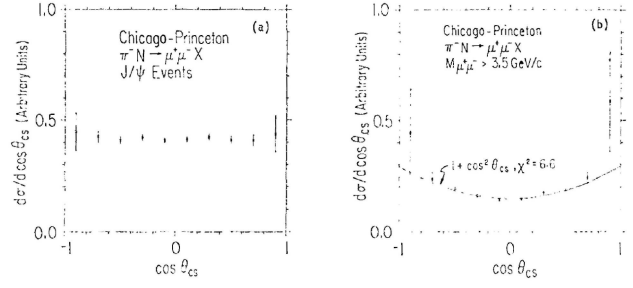


Fig. 5. Distribution of $d\sigma/d\cos\theta_{es}$ for (a) J/ψ events and (b) continuum pairs above the J/ψ for π^- -induced pairs at 225 GeV/c from ref. 2. The helicity angle θ_{es} is defined in the text.

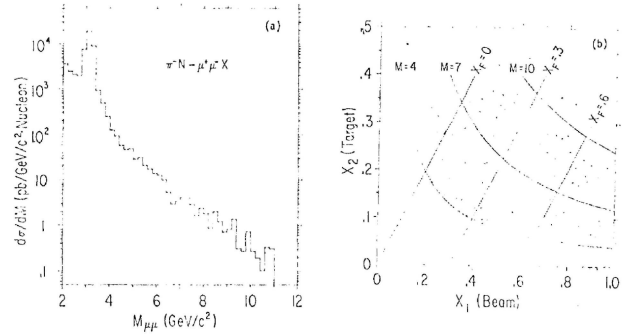


Fig. 6 a. Distribution of da/dM for $x_F > 0$ for π^- -induced muon pairs from ref. 2. Data above 4 GeV/c² was used to extract the pion structure function.

b. Scatter plot in x_1 and x_2 of the data used in the structure function fits.

Pion Structure Function

The general features of the muon pairs in the continuum are consistent with the Drell-Yan model. Assuming then that qq annihilation is the dominant process in the production of the continuum, one can extract information on the pion structure function. Data at 225 GeV/c are shown in Fig. 6a. In Fig. 6b is shown a scatter plot of the data in x_1 and x_2 the beam and target momentum fractions. In the region $x_1 > 0.2$ where the pion sea is negligible, the cross section for lepton pair production can be written as:

$$M^4 \frac{d\sigma}{dx_1 dx_2} = \frac{4\pi\alpha^2 s}{9} x_1 \bar{u}^\pi(x_1) \times \left[\frac{4}{9} x_2 u^N(x_2) + \frac{1}{9} x_2 \bar{d}^N(x_2) \right] \quad (1)$$

where

$$x_1 x_2 = M^2/s$$

$$x_1 - x_2 = x_F$$

and

$$x_1 \bar{u}^\pi(x_1) = x_1 d^\pi(x_1)$$

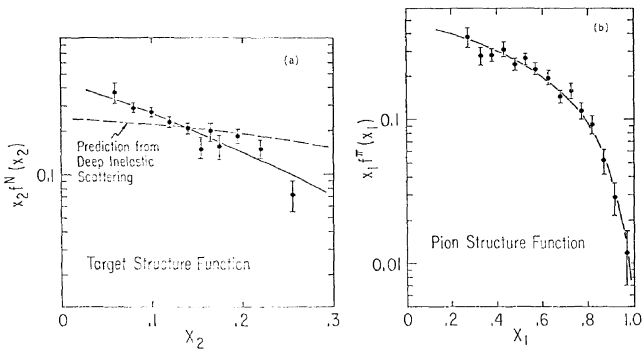


Fig. 7 a. The nucleon structure function $x_2^f(x_2) = 4/9x_2u^N(x_2) + 1/9x_2d^N(x_2)$. The shape is sensitive to the effects of transverse and quark mass (see the text),
 b. The pion structure function $X_i/\wedge x O^{\wedge i} \wedge C x_i) = X_l r f^*(X_l)$.

from isospin invariance and charge conjugation.

The cross section factors to a product of functions in x_{\pm} and x_2 . To test this hypothesis data was weighted by M^4 and binned in 16 intervals of x_x and 12 intervals of x_3 in the range $Jd > 0.2$, $0.05 < x_2 < 0.27$.

There were 141 populated bins which were fitted to 16 values representing the pion structure function and 12 values for the nucleon structure function. The results are shown in Figs. 7a and 7b where the nucleon term normalization has been set using the results from deep inelastic lepton scattering.⁷ The fit has a χ^2 of 133 for 113 degrees of freedom. The nucleon fit falls more rapidly than expected and is sensitive to the effects of p_T and quark mass. Two methods of including p_T effects were tried: (1) each quark was given a p_T vector of 1 GeV/c magnitude with their relative angles adjusted to produce the observed p_T , and (2) each quark was given half the observed p_T . Method (1) resulted in a negligible change in the pion structure function but resulted in a considerable flattening of the nucleon function. The resulting nucleon function gave a $(l-x)^a$ fit with $a=2.2$. Method (2) yielded a larger change in the pion structure function. The power of $(l-x)^*$ fit increased by 0.2 while the nucleon function changed only slightly.

Resonances above the $Jj < p$

Production of $0(3700)$ is clearly seen in π^- -N interactions at 225 GeV/c (Fig. 8). The branching fraction times cross section relative

to that for J/ψ production is given by

$$\frac{B\sigma_{\phi'}}{B\sigma_{J/\psi}} = 0.023 \pm 0.007$$

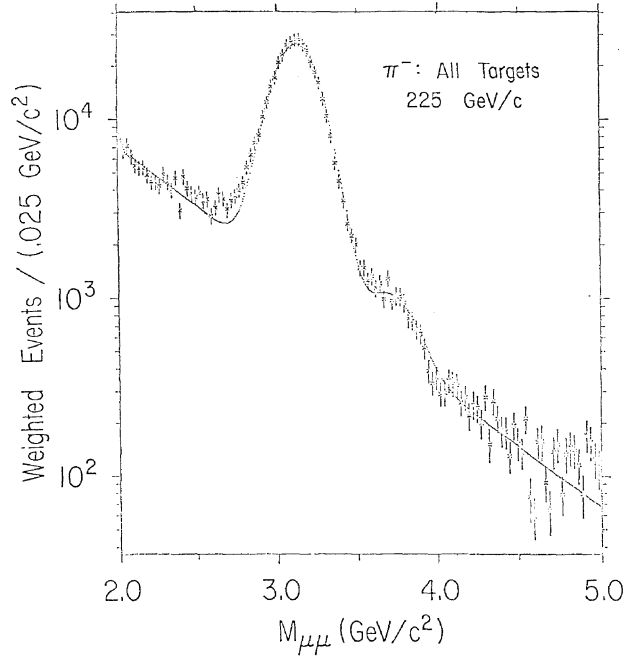


Fig. 8. Efficiency corrected muon pair effective mass distribution showing ($l >$ ' production (see text).

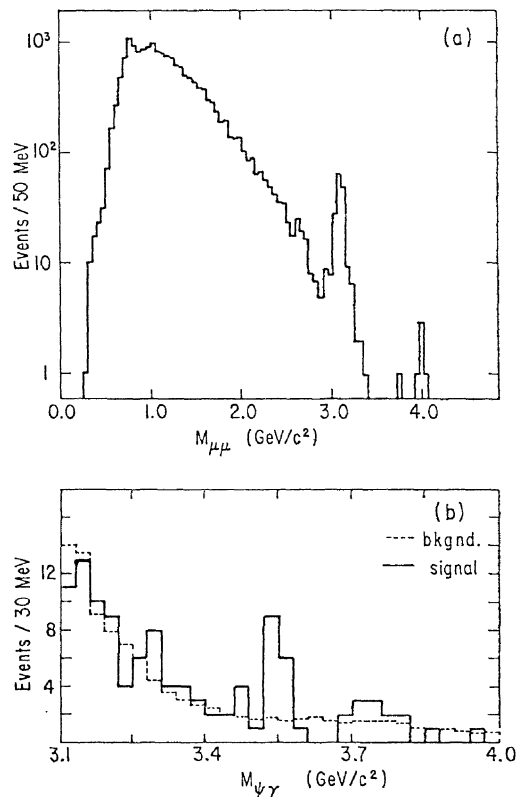


Fig. 9 a. Uncorrected muon pair effective mass distribution from ref. 8 showing $Jj(p$ production,
 b. The $J/\psi \rightarrow p\gamma$ effective mass distribution. A signal of 11 ± 4 events above background is seen in $3.55 \text{ GeV}/c^2$ (see text).

for $x > 0$. The result is similar to that previously reported in proton interactions at 400 GeV/c.⁸

New results for production of ρ states in π^-N interactions at 215 GeV/c from Fermilab are shown in Fig. 9.⁹ Figure 9a shows the muon pair signal observed. The spectrometer used has an open configuration and the distribution has not been corrected for background, however, a clear J/ψ signal can be seen. For events in the J/ψ peak where an accompanying photon is observed, the effective mass distribution of the $J/\psi \rightarrow \mu\mu$ system is shown in Fig. 9b. A signal of 11 ± 4 events above background is observed at 3.55 GeV/c². The cross section observed is given by:

$$\sigma_{\mu\mu} = 0.38 \pm 0.13$$

This is similar to the value 0.43 ± 0.21 obtained by Cobb *et al.*¹⁰ in proton-proton interactions at $\sqrt{s} = 55$ GeV. Mass resolution is not

sufficient to resolve between $\rho(3510)$ and $\rho(3550)$.

References

1. S. D. Drell and T. M. Yan: Phys. Rev. Letters 25 (1970) 316.
2. K. J. Anderson *et al.*: preprint submitted to this Conference EFI 78-38.
3. M.J. Corden *et al.*: Phys. Letters **76B** (1978) 226.
4. J. Alspector *et al.*: preprint submitted to this Conference BNL-OG419.
5. S. V. Golovkin *et al.*: preprint submitted to this Conference A10-287.
6. J. C. Collins and D. E. Soper: Phys. Rev. **D16** (1977) 2219.
7. We have used the parametrization suggested by Buras and Gaemers. A. J. Buras and K. J. F. Gaemers: Nucl. Phys. **B132** (1978) 249.
8. H. D. Snyder *et al.*: Phys. Rev. Letters 36 (1976) 1415.
9. L. Holloway *et al.*: preprint submitted to this Conference.
10. J. H. Cobb *et al.*: Phys. Letters **72B** (1978) 497.
11. D. M. Kaplan *et al.*: Results presented at the Vanderbilt Conference, March, 1978.

A10

Experiments at the IHEP-Serpukhov

A. A. DEREVSHCHIKOV

IHEP, Serpukhov

In this report the results of two experiments performed recently at IHEP (Serpukhov) are presented.

In the first experiment¹ an inclusive muon pair production process:

$$\pi^- + (\text{Cu nucleus}) \rightarrow \mu^+ \mu^- + X$$

In the continuum range $1.3 < A_{\mu\mu} < 2.5$ (GeV/c²) has been selected at $p_x = 21$ and 40 GeV/c. The experimental installation used for these measurements and other details were described in earlier paper, devoted to the investigation of the inclusive J/ψ -particle production processes in π^-N -collisions in the near-threshold range.²

To select the processes of prompt muon pair production in the continuum range one should reliably suppress the main background

processes: a) accidental background b) on-flight decays of two secondary $\pi(7T)$ -mesons with emission of muons, c) nuclear cascades that passed through the shielding and muon detector and misidentified as muons, d) interactions in the filter behind the target, e) "Tails" from ρ , a_1 , ϕ -meson and Λ -particle peaks.

To estimate the background from the muons, originating from $TC(K) \rightarrow LC$ decay and nuclear cascades we investigated the mass spectra of "muonic pairs" of identical sign ($\mu^+ \mu^+$, $\mu^- \mu^-$) and carried out special runs with a copper target of a reduced effective density and with a plastic glass target without a copper absorber. Moreover we carried out detailed investigation of the set up efficiency, track reconstruction procedure in the spectro-

Table I. Data on muon continuum $1.3 \leq M_{\mu^+\mu^-} \leq 2.5 \text{ GeV}/c^2$.

A.	Number of events and total cross sections		Notes				
	$p_\pi=27 \text{ GeV}/c$	$p_\pi=40 \text{ GeV}/c$					
$N(\mu^+\mu^-)$	201	173	a) The table presents $d\sigma/dM[X>0.3]$.				
$N(\mu^+\mu^-)+N(\mu^-\mu^+)$	1	5	b) $r=M^2_{\mu^+\mu^-}/s$.				
Upper limit for all background events in $N(\mu^+\mu^-)$	10%	15%	c) $M_{\mu^+\mu^-} \equiv M$ -muon pair effective mass.				
$\langle\sigma\rangle = \int_{1.3 \text{ GeV}}^{2.5 \text{ GeV}} d\sigma/dM[X_F>0.3]dM$	$74 \pm 8 \text{ nb}/(\text{Cu nucleus})$	$105 \pm 9 \text{ nb}/(\text{Cu nucleus})$	d) All cross sections are for Cu nucleus.				
B.	Differential cross sections						e) Statistic errors are indicated everywhere. The common systematic error of the scale is $\approx 20\%$.
$M(\mu^+\mu^-)$ (GeV/c^2)	$p_\pi=27 \text{ GeV}/c$			$p_\pi=40 \text{ GeV}/c$			
	r	$d\sigma/dM$ (n barn/ GeV)	$M^3 \cdot d\sigma/dM$ (n barn · GeV ³)	r	$d\sigma/dM$ (n barn/ GeV)	$M d\sigma/dM$ (n barn · GeV ²)	f) $x_F=p_{\parallel}/p_{\text{max}}$ (in c.m.s.).
1.3–1.6	0.035	148 ± 19	435 ± 57	0.028	203 ± 24	581 ± 66	
1.6–1.9	0.059	61 ± 18	321 ± 98	0.041	86 ± 14	467 ± 81	
1.9–2.2	0.081	29 ± 8	236 ± 69	0.056	36 ± 11	310 ± 96	
2.2–2.5	0.107	10 ± 4	127 ± 50	0.073	24 ± 8	302 ± 105	

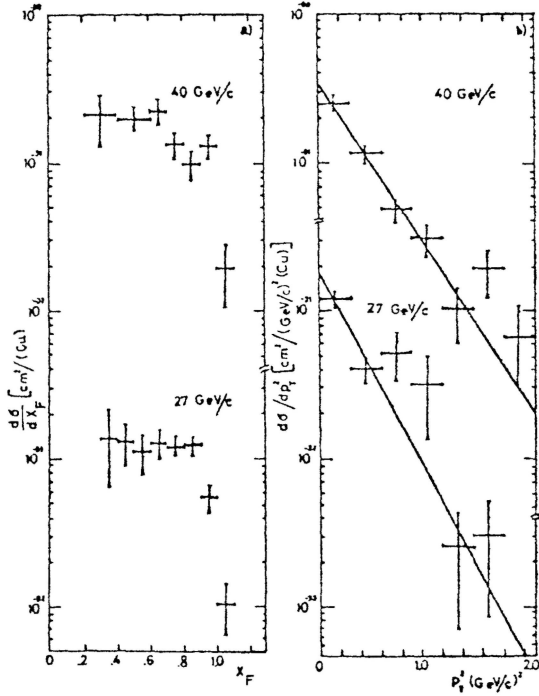


Fig. 1. (a) Differential cross section dependence for muon pair production in the muon continuum range $1.3 < M_{\mu^+\mu^-} < 2.5 \text{ GeV}/c^2$ on Cu nuclei on $x_F = p_{\parallel}/p_{\text{max}}$ (in the c.m.s.) for $p_\pi = 27$ and $40 \text{ GeV}/c$. (b) Differential cross section dependence for the same process $d\sigma/dp_T^2$ on the transverse momentum p_T .

meter, the methods of selection of the interactions in the target and all source of background processes.

The results of data handling and estimation of the upper limits for all the background

Table II. The Parameters of muon pair distributions with masses $1.3 \leq M_{\mu^+\mu^-} \leq 2.5 \text{ GeV}/c^2$ over variables $x_F = p_{\parallel}/p_{\text{max}}$ and p_T (in c.m.s.).

	$p_\pi=27$ GeV/c	$p_\pi=40$ GeV/c	
$d\sigma/dp_T^2 = Ae^{-bp_T^2}$	b (GeV/c) ⁻²	$2.9^{+0.4}_{-0.3}$	2.2 ± 0.3
$(E/p_{\text{max}})d\sigma/dx_F = C(1-x_F)^{n_1} \times (1+x_F)^{n_2}$	n_1	$0.67^{+0.17}_{-0.15}$	$0.20^{+0.17}_{-0.14}$
	n_2	5.4 ± 0.5	2.1 ± 0.5
$d\sigma/dx_F = B(1-x_F)^{m_1} \times (1+x_F)^{m_2}$	m_1	0.65 ± 0.15	$0.18^{+0.17}_{-0.07}$
	m_2	3.5 ± 0.5	0.1 ± 0.5

events are listed in Table I. Figure 1 illustrates the distribution of the relevant cross sections in the kinematic variables x_F and p_T . The main characteristics of these distributions are quoted in Table II.

The data on average value for the transverse momentum $\langle p_T \rangle$ as a function of dimuon system mass for the whole effective mass range, that was investigated, are also of interest (Fig. 2a). There is an evident growth of the values for $\langle p_T \rangle$ with an effective mass increase that is in agreement with the experiments performed at higher energies. From the comparison of the data on average values for the transverse momentum for fixed intervals of effective masses of muon pairs at different incident energies one comes to a conclusion on the

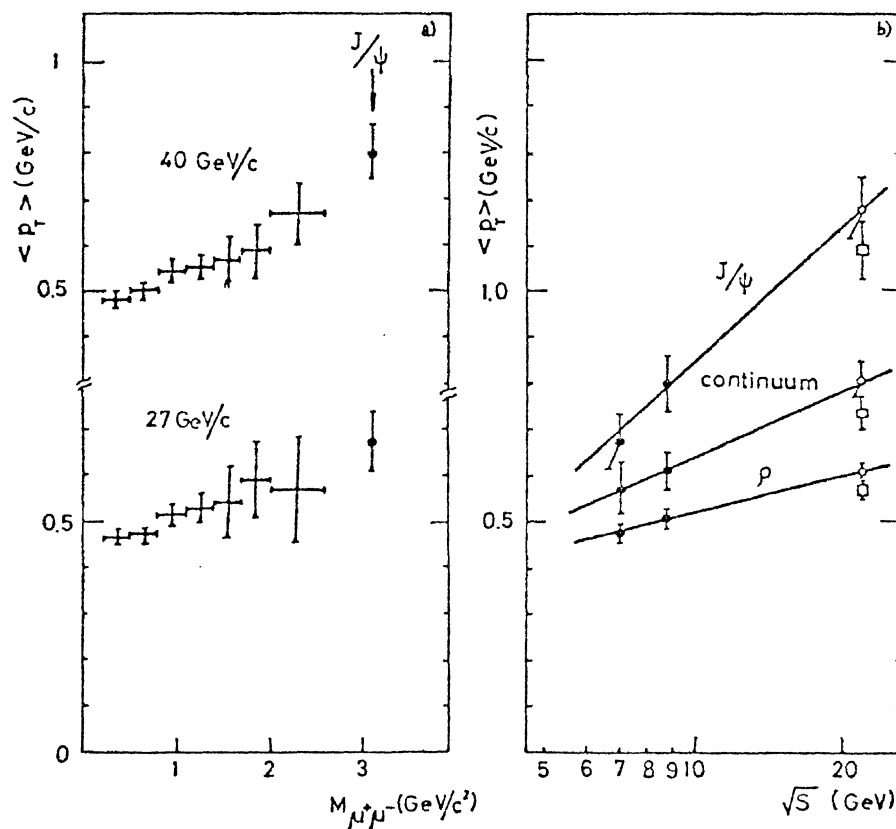


Fig. 2. (a) The dependence of the average value for the transverse momentum $\langle p_T \rangle$ on muonic pair mass in the whole mass range, investigated with the set up "LE.PTON" for $p_K=27$ and $40 \text{ GeV}/c$. All the data correspond to $x^A > 0.3$. (b) The dependence of the average value for the transverse momentum of muonic pair $\langle p_T \rangle$ on incident energy for a fixed mass value: 1) J/ψ particle range ($2.6 < M_{\mu^+\mu^-} < 3.6 \text{ GeV}/c^2$); 2) the continuum range ($1.3 < M_{\mu^+\mu^-} < 2.5 \text{ GeV}/c^2$); 3) ρ -meson range ($0.5 < M_{\mu^+\mu^-} < 1.0 \text{ GeV}/c^2$).

When comparing the data of the two experiments one should bear in mind different measurement conditions: 1) the result of the present work is related to the Cu nucleus and the range $x^A > 0.3$; 2) the result from work² is related to the C nucleus and the range $x^A < 0.15$. As is known, under all other equal conditions $\langle r \rangle$ is somewhat smaller for C nuclei than for Cu ones. This fact has been taken into account in figure. The transfer for heavier nuclei was made on the basis of the data from ref. 2 for carbon and Sn. (+ — the results of this work; § — the results from ref. 2; 6 — the results from ref. 2 with a correction for the transfer from C target to Cu one.

increase of the transverse momentum with energy growth.

If the processes of muon pair production follow the Drell-Yan model, then the expected cross sections will have a scaling dependence. Fig. 3 presents our data together with the results from other works on muon continuum in $\gamma\gamma$ -N-interaction. The behaviour of dimuon state spectra does not contradict scaling and the values for the cross sections are in the order of magnitude in agreement with the theoretical estimates; however the measurement accuracy and the amount of the data are not sufficient.

In the second experiment⁵ the values for the ratio of prompt positron to π^+ -mesons (R_e) ($p_{\pm} = 1.2-2.8 \text{ GeV}/c^2$) produced from interaction of the 70 GeV internal proton beam with a thin (1 JJ) carbon film, have been measured.

The experimental set up was a simple spectrometer with a proportional chambers and Cerenkov counters, that allows to identify the secondary particles. The corrections connected with particle absorption in the beam channel, were determined in special experiments with an accuracy of $\sim 1\%$ when the values for R_e were measured at different

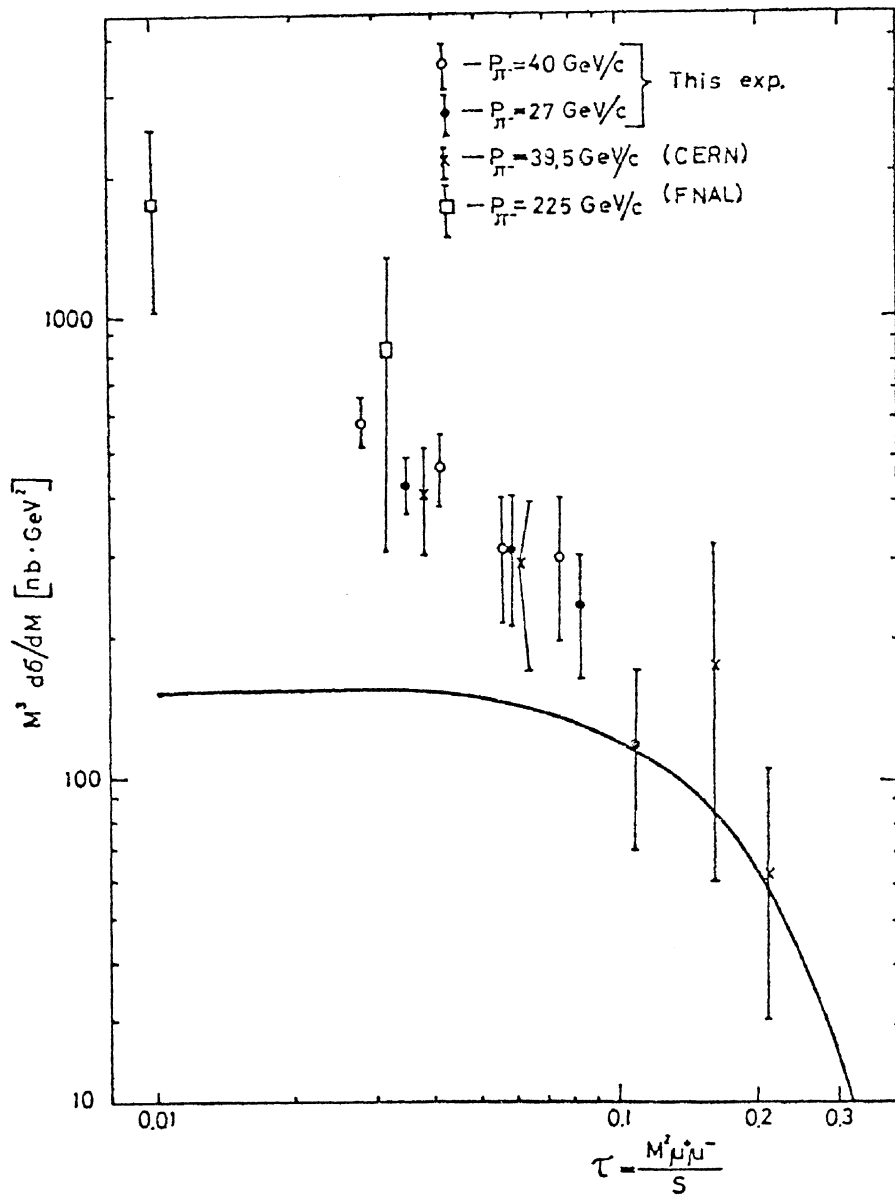


Fig. 3. The dependence $M^* \frac{d\sigma}{dM} [\text{nb} \cdot \text{GeV}^2]$ on the scaling variable $\tau = M_{\beta^+ \beta^-}^2 / S$. In figure we present the comparison of the results from the present work with those from (FNAL)² and preliminary data of CERN-Q (Budapest, July, 1978). All the data are reduced for the range $x^A > 0.3$ corresponding to the measurements of our work and related to Cu nuclei in assumption on the cross section linear dependence on A. The solid curve reflects the theoretical estimate of $M^* \frac{d\sigma}{dM} (\beta^+ \beta^-)$ in the Drell-Yan model for parametrization of the hadronic structure functions according to ref. 3.

amount of the matter in the beam channel and then extrapolated to a zero thickness. To define the value for the direct component of positron, one has to reduce the contribution from the Dalitz decay of $\gamma c^0(\pi^0)$. Figure 4 presents the value for R_e after all the corrections together with the data on the yields of "prompt" π^- -mesons from paper.⁶

The results in Fig. 4 indicate that within the interval of $p_{\pi^\pm} \sim (1-3)$ GeV/c the direct com-

ponent of electrons R_e is $\sim 3 \cdot 10^{-5}$ and differs quite noticeably from the same value for muons $i^? \sim (7 \pm 1) \cdot 10^{-5}$. The available set of experimental data is in favour of the fact, that charmed mesons may be a source for prompt leptons. In this case the only source for prompt electrons is semileptonic decays of the parents and for prompt muons both two particle decays and semileptonic decay of the parents.

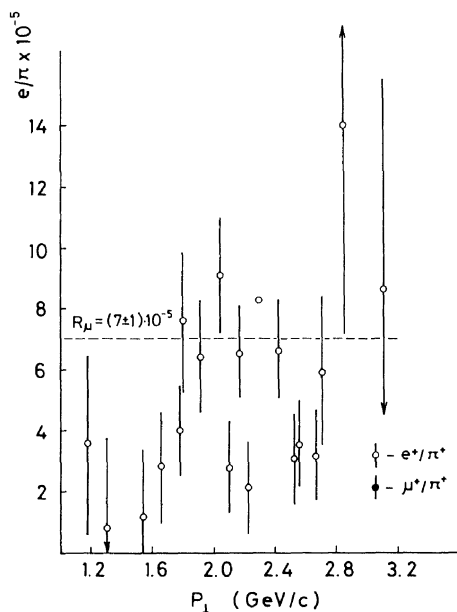


Fig. 4.

References

1. S. Y. Golovkin *et al.*: Preprint IHEP 78-18, Serpukhov, 1978 (contributed paper No. 287).
2. Yu. B. Bushnin *et al.*: Preprint IHEP 71-93, Serpukhov, 1977; Phys. Letters **72B** (1977) 269.
3. J. G. Branson *et al.*: Phys. Rev. Letters 38 (1977) 1334.
4. A. Donnachie and P. V. Landshoff: Nucl. Phys. **B112** (1976) 233.
5. S.A. Akimenko *et al.*: contributed paper No. 947.
6. Y. Y. Abramov *et al.*: Int. Conf., London, 1974.

PROC. 19th INT. CONF. HIGH ENERGY PHYSICS
TOKYO, 1978

A 10 Direct Electron Production in 10 GeV Region

T. KITAGAKI

Tohoku University

The direct electron production in 10 GeV region is thought to be a somewhat different problem from those in high energy region. The source origin of these electrons at low energy and small P_T region might be hadron Bremsstrahlung. There were five contributions on this subject.

1. #460. Minnesota, Argonne, Rice and Columbia Collaboration made a search for direct electron production in p-p and p-Be interaction at 12 GeV/c. Electrons were measured using a single arm spectrometer at four center of mass angles, $0^\circ=20, 35, 63,$ and 84° , which were set by changing the target position. Figure 1 shows the e/π ratios from this experiment, where the solid data points are for e^- and open points for e^+ . The contribution from Dalitz decays of TZ, ρ^0 and ϕ^0 were subtracted. The solid curve represents the contribution of electron pair decays from

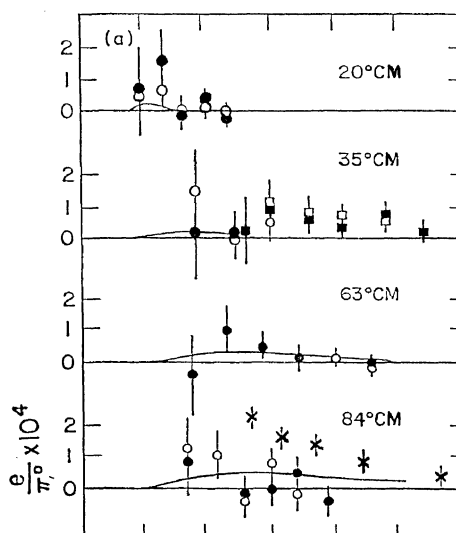


Fig. 1. Rate of direct electron production versus JTT . Solid data points are for e^- , open points for e^+ . Circles and squares represent data from beryllium and hydrogen targets, respectively. The crosses are the data of ref. 1. The lines are estimates of the vector meson contribution [No. 460, Minnesota],

vector mesons. They conclude that the production of electron is competitive with the vector meson background. The rate was $e/rr = (0.30 \pm 0.20) \times 10^{-4}$ at $\theta^* = 84^\circ$.

2. #407. The direct electron search in p-Be interactions at 9 GeV/c is being held at KEK using a double arm spectrometer. (KEK, Osaka City, I.N.S., Kyoto, Tokyo, Saitama Collaboration).

3. #553. Another direct electron production experiment in p-p 8 GeV/c has been made at KEK using the KEK 1 m Hydrogen Bubble Chamber (Tohoku, Tohoku Gakuin, Nara, KEK Collaboration). Four Ta plates, 1.5, 2.0, 3.0 and 3.0 mm (0.7 radiation length), were installed in the chamber and one million pictures were taken. Events with two identified unlike charge electrons were collected.

All signatures observed in the bubble chamber pictures, such as spiraling, bubble density, Bremsstrahlung in hydrogen and shower in Ta plates, were used for the electron identification. Background due to real photon pair conversion and large angle scatterings of Dalitz pair electrons in liquid hydrogen very near the vertices were checked and estimated to be less than 0.1 events in the nine high mass electron pairs with $M(ee) > 140$ MeV. Hadron contamination is also estimated to be less than 0.02 events under this experimental condi-

tion. Figure 2 shows the mass distribution of

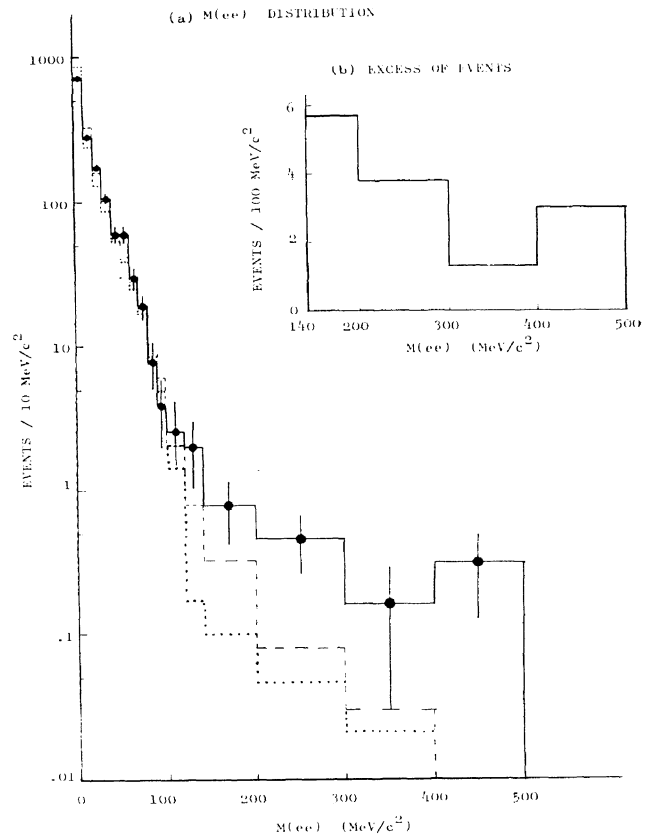


Fig. 2. Mass distribution of e^+e^- pairs for (a) all events. The dashed histogram shows the simulation for Dalitz pair events from TZ^0 , rf and co^0 . The dotted one shows the simulation neglecting the experimental resolution, (b) Excess events over the dashed histogram, corrected for detection efficiency [No. 553, Tohoku].

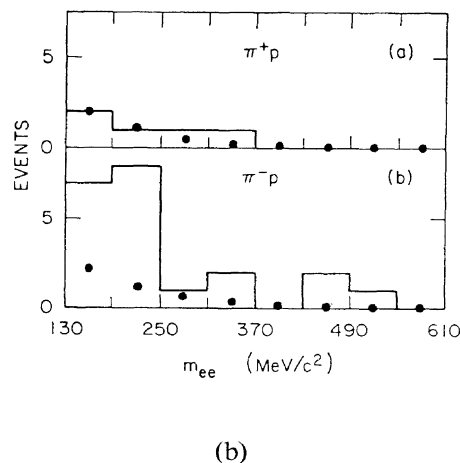
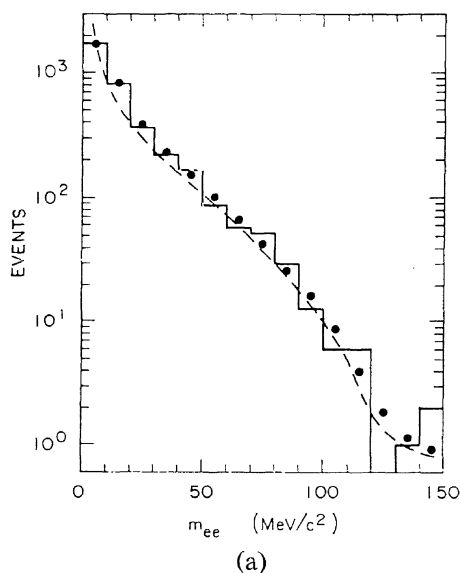


Fig. 3 (a). Mass distribution of e^+e^- pairs from π^+p and $7r\sim p$, both electrons identified. The dots represent the simulation, and dashes the simulation without the effects of resolution, (b). Observed (lines) and expected (dots) events at higher masses for $T\pi^+p$, and $7i\sim p$ [No. 602, SLAC].

the electron pairs. The dashed histogram is the results of a Monte Carlo simulation for Dalitz decays from $TZ \setminus rf$ and OJ^0 with the experimental resolution. Contributions from other known particle decays are less than 1/3 of the Dalitz pair contribution from rf and o^0 for $M(ee) > 140$ MeV. The excess of electron pairs above $M(ee) > 140$ MeV is found to be $e/7r = (1.4 \pm 0.7) \times 10^{-4}$ after subtracting the known backgrounds.

4. #602. SLAC, Duke, Imp. C Collaboration made similar experiments using the SLAC 40" HBC with three Ta plates, 1 radiation length each. $7r^+p$ and $rc \sim p$ pictures were taken at 18 GeV/c with triggering by interactions. The sample includes 4.2×10^5 and 5.2×10^5 of inelastically produced secondary IT^* for $7T^+p$ and $7r \sim p$ respectively. e^+e^-

pairs both electrons identified were collected and the results are shown in Fig. 3. In $7T^+p$ interactions, no significant excess was observed and, $e/7r \sim 2.5 \times 10^{-5}$ for $M(ee) > 100$ MeV. In $7r \sim p$, however, they found 16 heavy pairs and the $e/7r$ ratio to be $(0.87 \pm 0.25) \times 10^{-4}$ which was an excess not explained by known meson decays. Figure 4 shows the comparison of $e/7r$ ratios as a function of $P_T(\epsilon)$ for the Tohoku and SLAC data together with the Penn., Stony Brook data.¹

5. #628. Duke, SUNY, Albany reported the observation of f_s 's not associated with n^0 or rf in the $7r^+p$ interactions at 15 and 10.5 GeV/c. Figure 5 shows the Feynman X distribution of f_s and the P_T distribution with the cut $0 < A^+ < 0.01$. Figures show the excess of j over the simulation calculation for

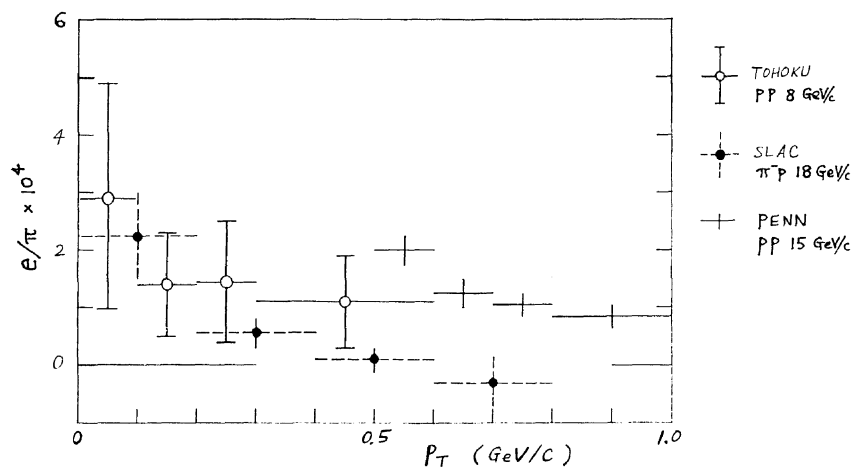


Fig. 4. The comparison of the $e/7r$ ratios versus P_T .

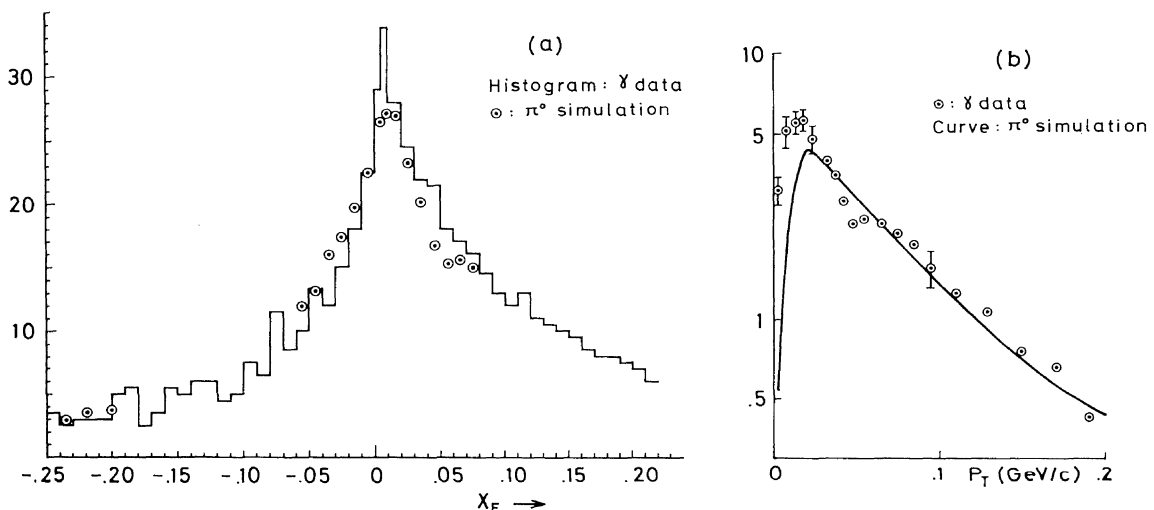


Fig. 5 (a). The Feynman X distribution of the f_s produced in $;\pi^+p$ collisions at 15 GeV/c. (b). P_T distribution of f_s produced in $;\pi^+p$ collisions in a H_2 -Ne mixture at 10.5 GeV/c. The events have been restricted so that the f_s have a small, positive X value [No. 628, Duke].

the π 's at small X and small P_T region. They concluded that 0.9 % of all y is not associated with π^0 or y_f .

Reference

1. E. W. Beier *et al*: PRL 37 (1976) 1117.